Gas-phase Dynamics of Collision Induced Unfolding, Collision Induced Dissociation and Electron Transfer Dissociation-activated Polymer Ions

Jean R. N. Haler[1], Philippe Massonnet[1], Johann Far[1], Victor R. de la Rosa[2], Philippe Lecomte[3], Richard Hoogenboom[2], Christine Jérôme[3], Edwin De Pauw[1]*

[1]Mass Spectrometry Laboratory, University of Liège, MolSys Research unit, Quartier Agora, Allée du Six Aout 11, B-4000 Liège, Belgium

[2]Supramolecular Chemistry Group, Centre of Macromolecular Chemistry (CMaC), Department of Organic and Macromolecular Chemistry, Ghent University, Krijgslaan 281 S4, B-9000 Ghent, Belgium

[3]Center for Education and Research on Macromolecules, University of Liège, CESAM Research unit, Quartier Agora, Allée du Six Aout 13, B-4000 Liège, Belgium

*Corresponding author email address: jean.haler@uliege.be

Supporting Information

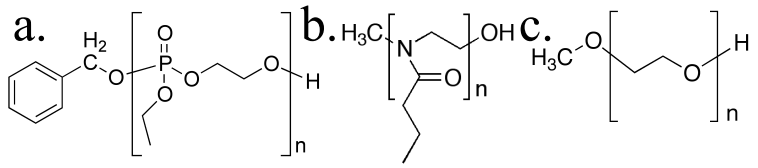

Figure SI1: Representations of the three polymers used in this study: a. PEtP poly(ethoxy phosphate) or poly(2-ethoxy-1,3,2-dioxaphospholane 2-oxide); b. P*n*-PrOx poly(2-n-propyl-2-oxazoline); c. PEO poly(ethylene oxide) monomethyl ether

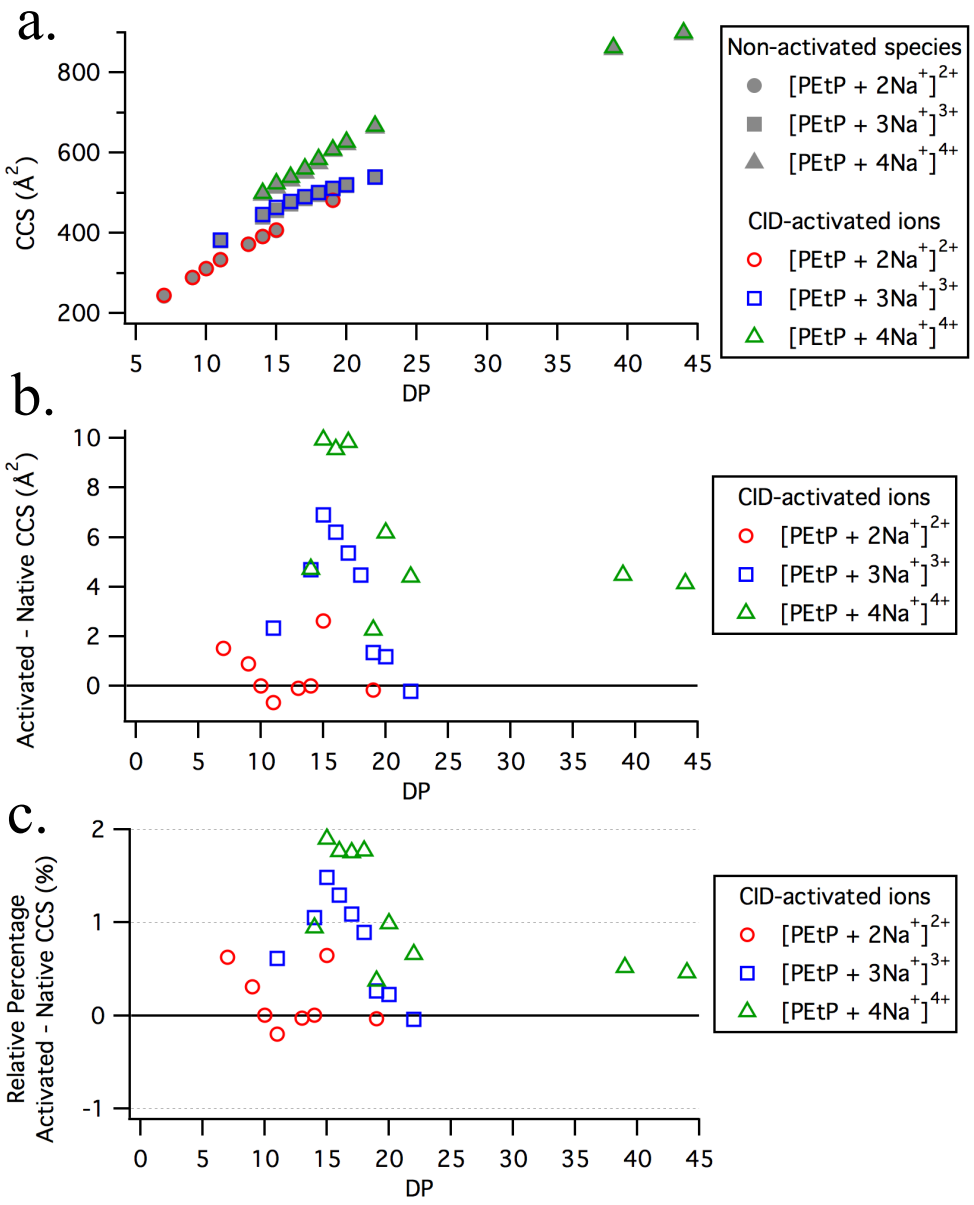

Figure SI2: Collisional activation of precursor ions. a. CCS plotted as a function of the DP for 3 charge states of PEtP. Gray markers represent native non-activated precursor ions and colored markers represent collisionally-activated precursor ions. b. CCS difference between activated and non-activated polymer complexes. c. Percentage CCS deviations of activated and non-activated polymer complexes (Equation 1 with CCS instead of t_d).

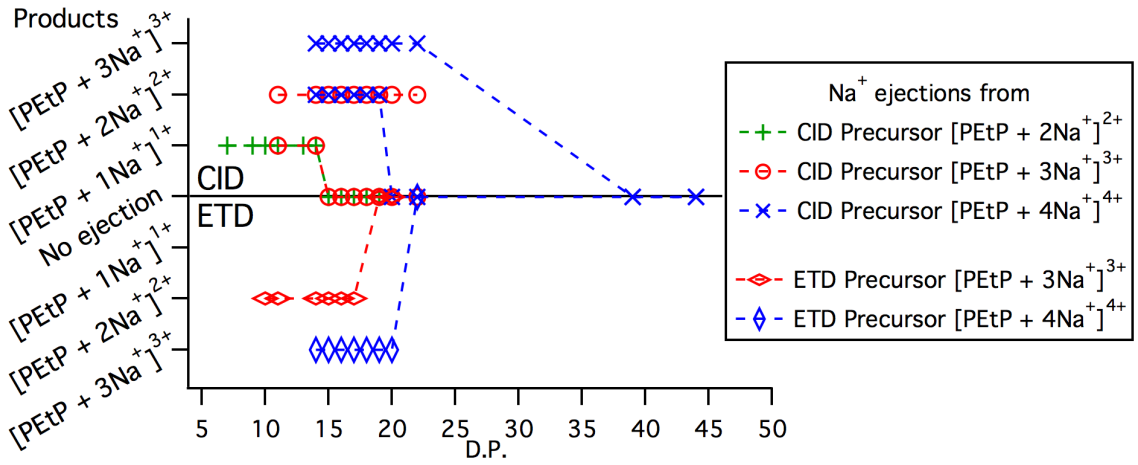

Figure SI3: PEtP cation ejection species formed (left axis) from different precursor ions (legend) according to the charge state and the DP. The top part of the plot represents the species formed using CID. 2+, 3+ and 4+ precursor ions are sampled for CID. The bottom part of the plot accounts for the ETnoD-formed species. The 2+ precursor ions do not react using ETD; only the 3+ and 4+ precursor ions are represented in the plot for ETD.

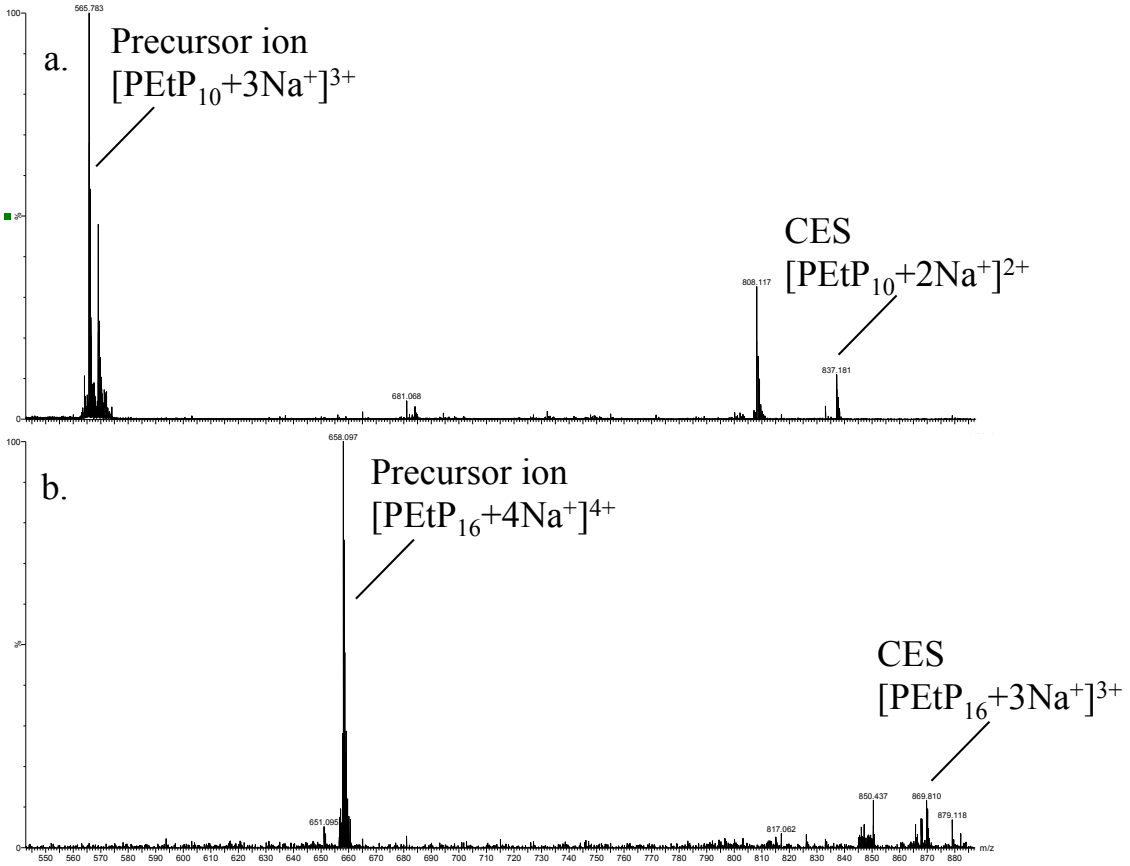

Figure SI4: ETD spectra of a. $[PEtP_{10} + 3Na^+]^{3+}$ precursor ion and b. $[PEtP_{16} + 4Na^+]^{4+}$ precursor ion. The CES (cation ejection species) from one cation ejection yields one of the most intense signals.

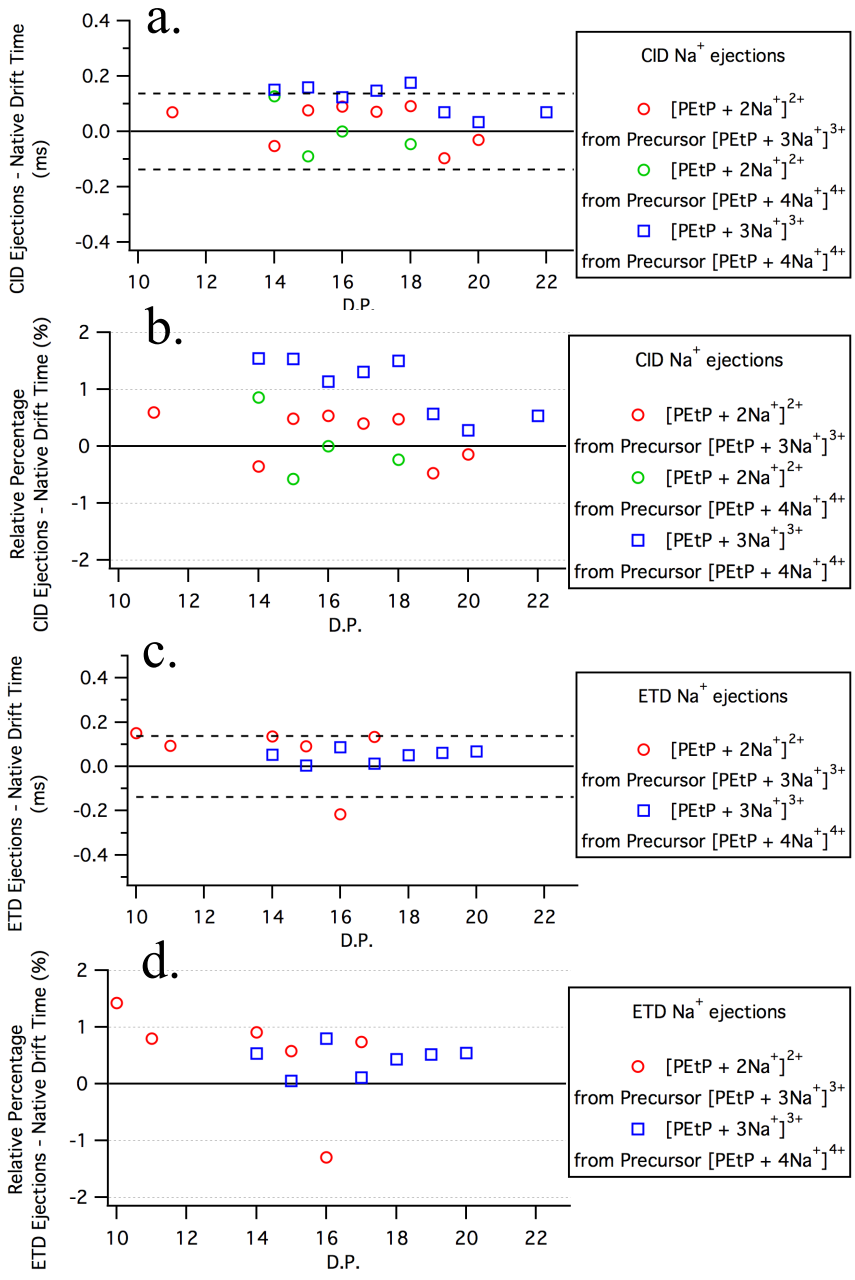

Figure SI5: Drift time (t_d) differences and percentage deviations of the CID (a. and b.) and ETnoD (c. and d.) formed cation ejection species compared to the native non-activated ions (see Equation 1), plotted as a function of the DP for different charge states. 2+ ions are formed from both 3+ and 4+ precursor ions. 3+ ions are formed from 4+ precursor ions. The dotted lines in a. and c. represent the instrument's acquisition bin width.

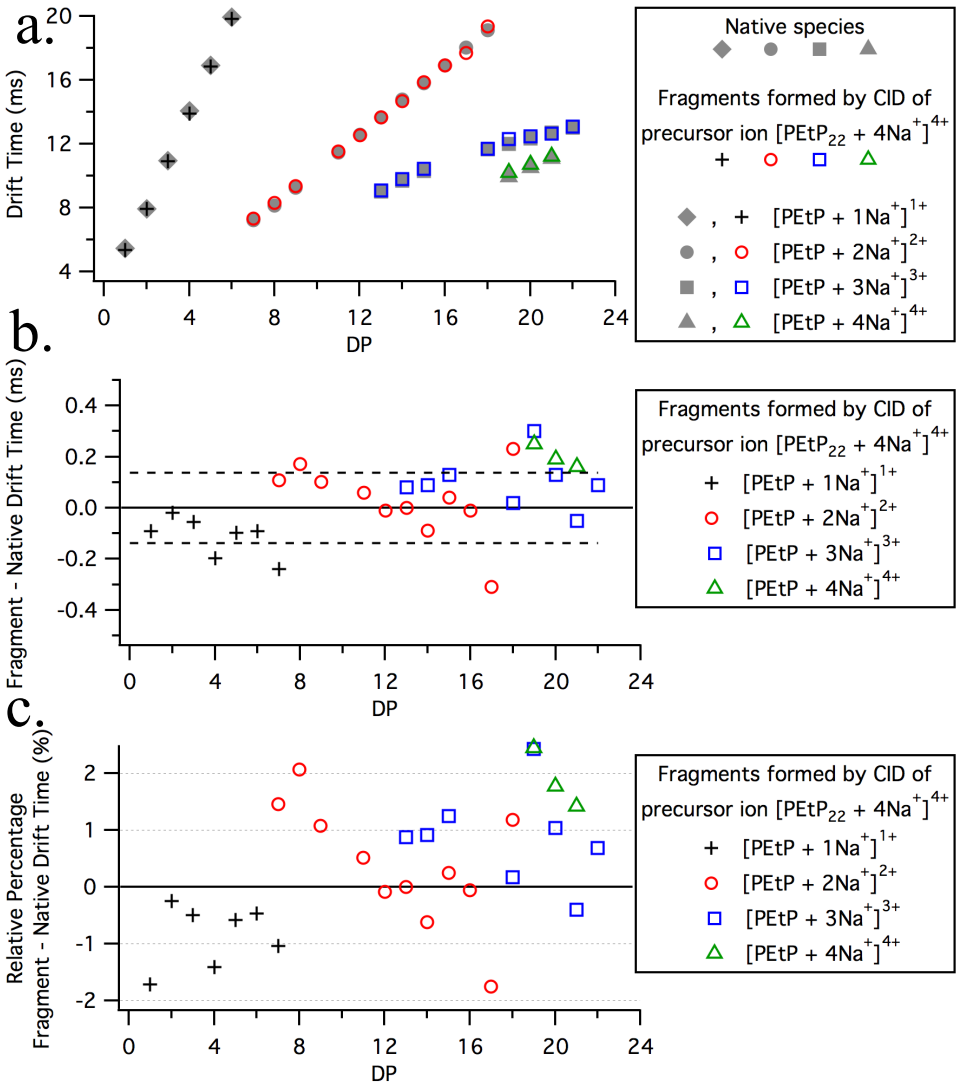

Figure SI6: Comparison of CID-obtained fragment ions from the $[PEtP_{22} + 4Na^+]^{4+}$ precursor ion with native intact polymer ions as a function of the DP. The analyzed fragment ions yield *m/z* values identical to smaller intact polymer ions. a. Drift times plotted as a function of the DP. Gray markers represent native intact polymer ions and colored markers represent fragment ions. b. Drift time difference between fragment ions and native intact polymer ions. The dotted lines represent the instrument's acquisition bin width. c. Percentage drift time deviations of fragment ions and native intact polymer ions (Equation 1).

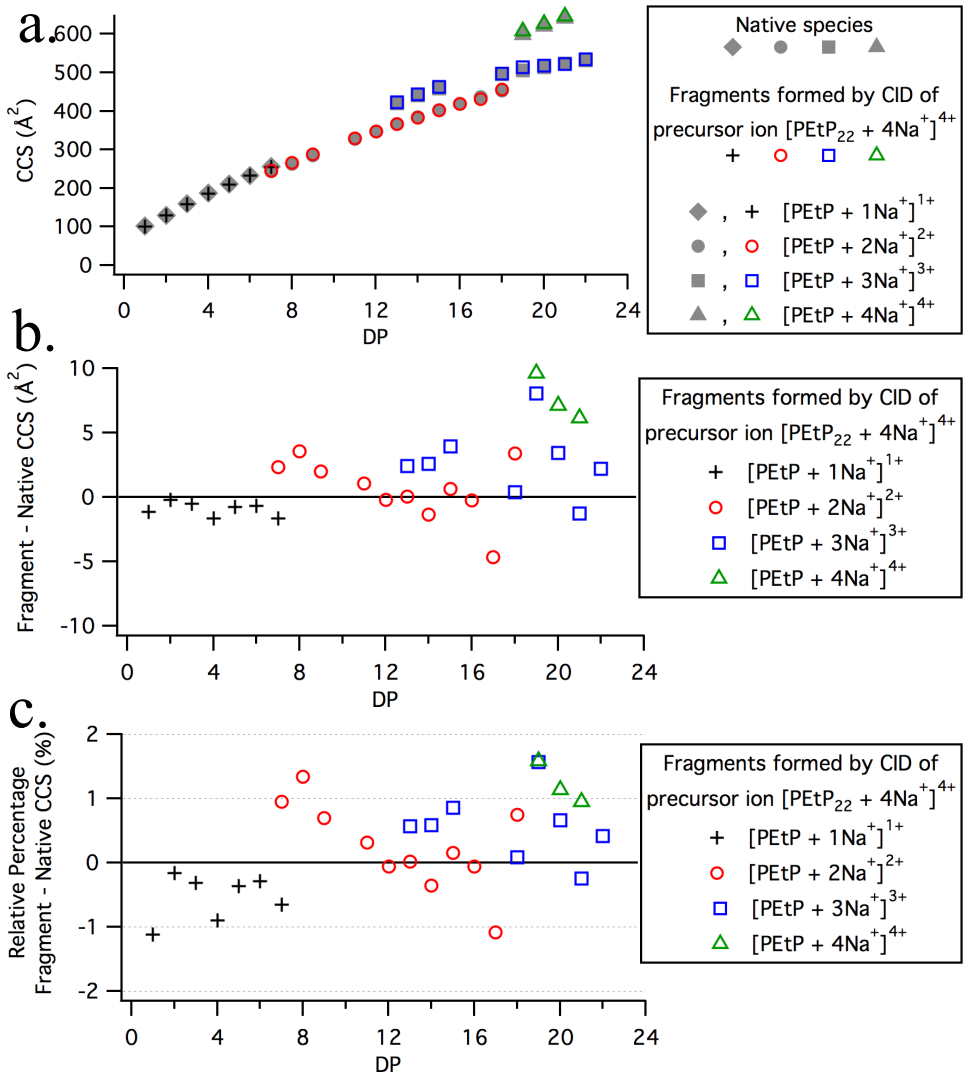

Figure SI7: Comparison of CID-obtained fragment ions from the $[PEtP_{22} + 4Na^+]^{4+}$ precursor ion with native intact polymer ions as a function of the DP. The analyzed fragment ions yield *m/z* values identical to smaller intact polymer ions. a. CCS plotted as a function of the DP. Gray markers represent native intact polymer ions and colored markers represent fragment ions. b. CCS difference between fragment ions and native intact polymer ions. c. Percentage CCS deviations of fragment ions and native intact polymer ions (Equation 1 with CCS instead of t_d).

Table SI1: t_d and CCS percentage deviations of fragment ions from $[PEtP_{22} + 4Na^+]^{4+}$ compared to their native (intact) counterparts (Equation 1 for either t_d or CCS). The analyzed species correspond to ions having *m/z* values of depolymerized polymer ions, without assuming that the fragment ions are solely formed by depolymerized ions. Figures SI6 and SI7 represent the plots of the t_d and CCS evolutions, their differences and their percentage deviations. The t_d of most fragment ions is beyond the limiting acquisition bin width (Figure SI6.b.).

Fragments from precursor ion $[PEtP_{22}+4Na^+]^{4+}$								
DP	$[M+1Na^+]^{1+}$		$[M+2Na^+]^{2+}$		$[M+3Na^+]^{3+}$		$[M+4Na^+]^{4+}$	
	% dt	% CCS	% dt	% CCS	% dt	% CCS	% dt	% CCS
1	-1.71	-1.12						
2	-0.24	-0.16						
3	-0.50	-0.32						
4	-1.41	-0.90						
5	-0.58	-0.37						
6	-0.46	-0.29						
7	-1.04	-0.66	1.46	0.95				
8			2.07	1.34				
9			1.08	0.70				
11			0.52	0.32				
12			-0.08	-0.06				
13			0.00	0.01	0.88	0.57		
14			-0.61	-0.35	0.92	0.59		
15			0.25	0.15	1.25	0.85		
16			-0.06	-0.06				
17			-1.75	-1.08				
18			1.19	0.74	0.17	0.08		
19					2.44	1.57	2.45	1.59
20					1.04	0.66	1.77	1.14
21					-0.40	-0.24	1.42	0.95
22					0.69	0.41		

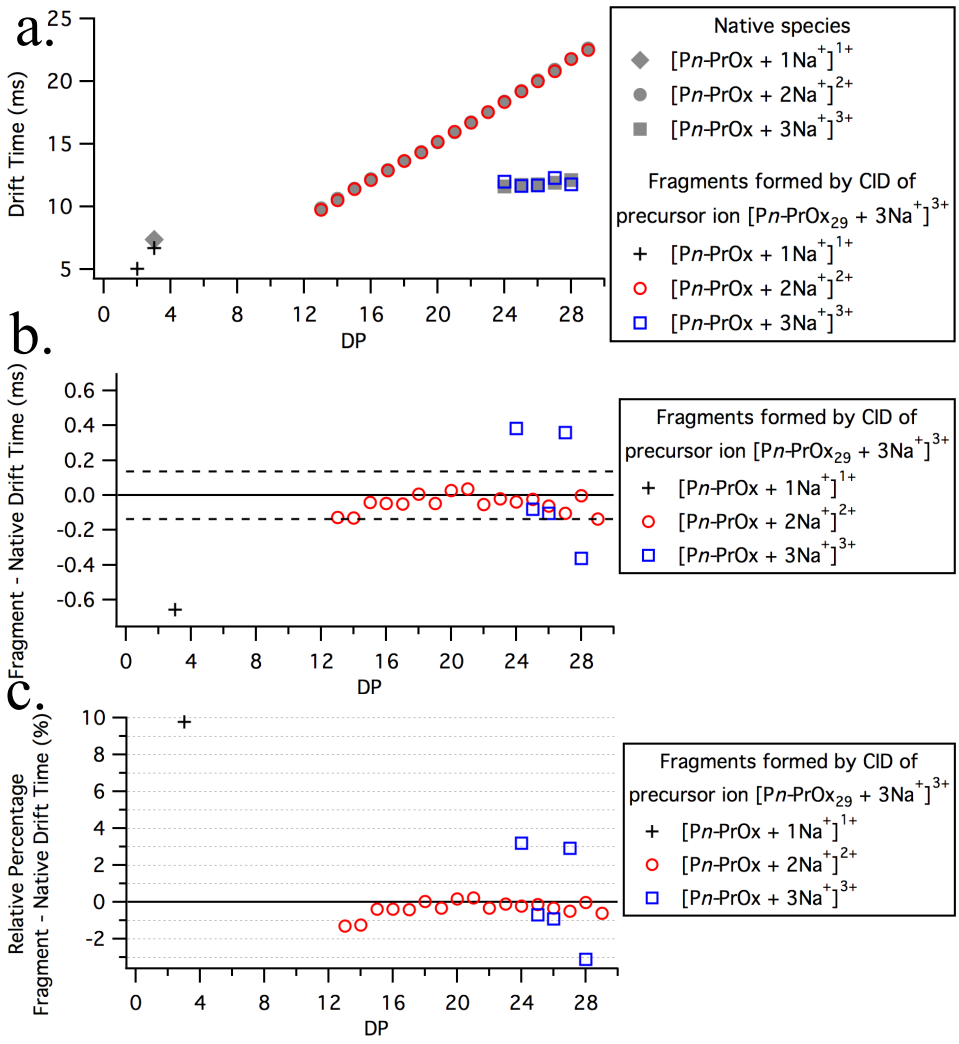

Figure SI8: Comparison of CID-obtained fragment ions from the $[Pn\text{-}PrOx_{29} + 3Na^+]^{3+}$ precursor ion with native intact polymer ions as a function of the DP. The analyzed fragment ions yield *m/z* values identical to smaller intact polymer ions. a. Drift times plotted as a function of the DP. Gray markers represent native intact polymer ions and colored markers represent fragment ions. b. Drift time difference between fragment ions and native intact polymer ions. The dotted lines represent the instrument's acquisition bin width. c. Percentage drift time deviations of fragment ions and native intact polymer ions (Equation 1).

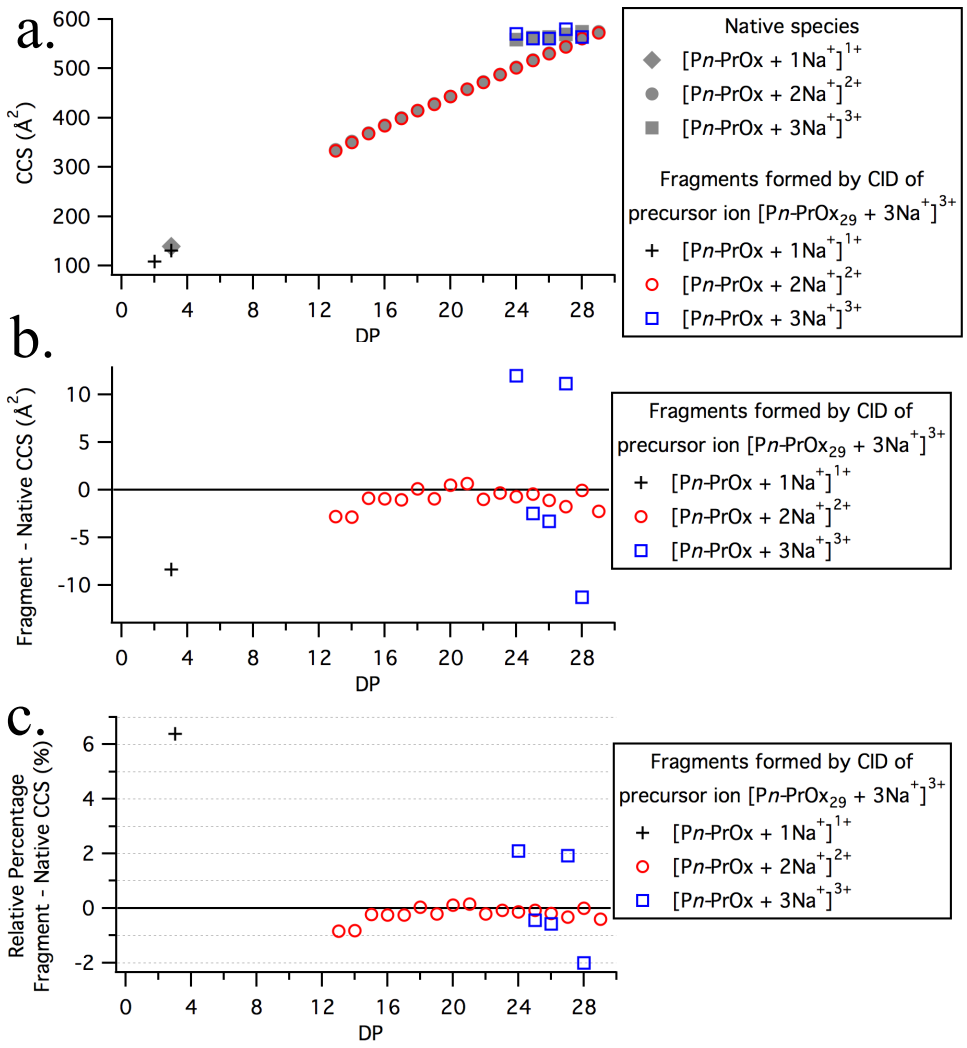

Figure SI9: Comparison of CID-obtained fragment ions from the $[Pn\text{-}PrOx_{29} + 3Na^+]^{3+}$ precursor ion with native intact polymer ions as a function of the DP. The analyzed fragment ions yield *m/z* values identical to smaller intact polymer ions. a. CCS plotted as a function of the DP. Gray markers represent native intact polymer ions and colored markers represent fragment ions. b. CCS difference between fragment ions and native intact polymer ions. c. Percentage CCS deviations of fragment ions and native intact polymer ions (Equation 1 with CCS instead of t_d).

Table SI2: t_d and CCS percentage deviations of fragment ions from $[P\textit{n}\text{-}PrOx_{29} + 3Na^+]^{3+}$ compared to their native (intact) counterparts (Equation 1 for either t_d or CCS). The analyzed species correspond to ions having *m/z* values of depolymerized polymer ions, without assuming that the fragment ions are solely formed by depolymerized ions. Figures SI8 and SI9 represent the plots of the t_d and CCS evolutions, their differences and their percentage deviations. The t_d of most fragment ions is beyond the limiting acquisition bin width (Figure SI8.b.).

Fragments from precursor ion $[PnPrOx_{29}+3Na^+]^{3+}$						
DP	$[M+1Na^+]^{1+}$		$[M+2Na^+]^{2+}$		$[M+3Na^+]^{3+}$	
	% dt	% CCS	% dt	% CCS	% dt	% CCS
3	9.79	6.39				
13			-1.30	-0.85		
14			-1.25	-0.82		
15			-0.37	-0.24		
16			-0.38	-0.25		
17			-0.40	-0.26		
18			0.04	0.03		
19			-0.34	-0.22		
20			0.18	0.11		
21			0.23	0.15		
22			-0.33	-0.21		
23			-0.11	-0.07		
24			-0.21	-0.14	3.20	2.10
25			-0.13	-0.08	-0.68	-0.45
26			-0.32	-0.20	-0.90	-0.59
27			-0.50	-0.33	2.93	1.92
28			-0.02	-0.01	-3.09	-2.01
29			-0.61	-0.40		

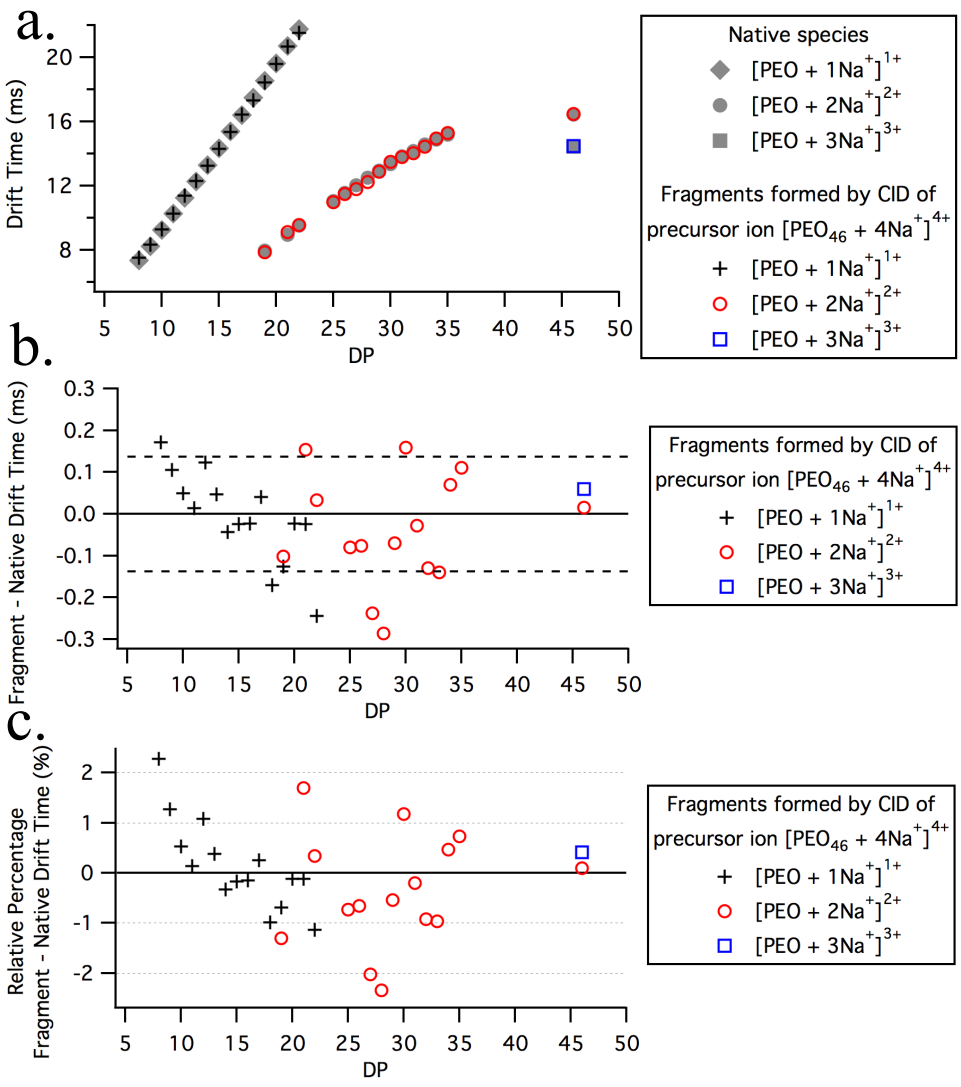

Figure SI10: Comparison of CID-obtained fragment ions from the $[PEO_{46} + 4Na^+]^{4+}$ precursor ion with native intact polymer ions as a function of the DP. The analyzed fragment ions yield *m/z* values identical to smaller intact polymer ions. a. Drift times plotted as a function of the DP. Gray markers represent native intact polymer ions and colored markers represent fragment ions. b. Drift time difference between fragment ions and native intact polymer ions. The dotted lines represent the instrument's acquisition bin width. c. Percentage drift time deviations of fragment ions and native intact polymer ions (Equation 1).

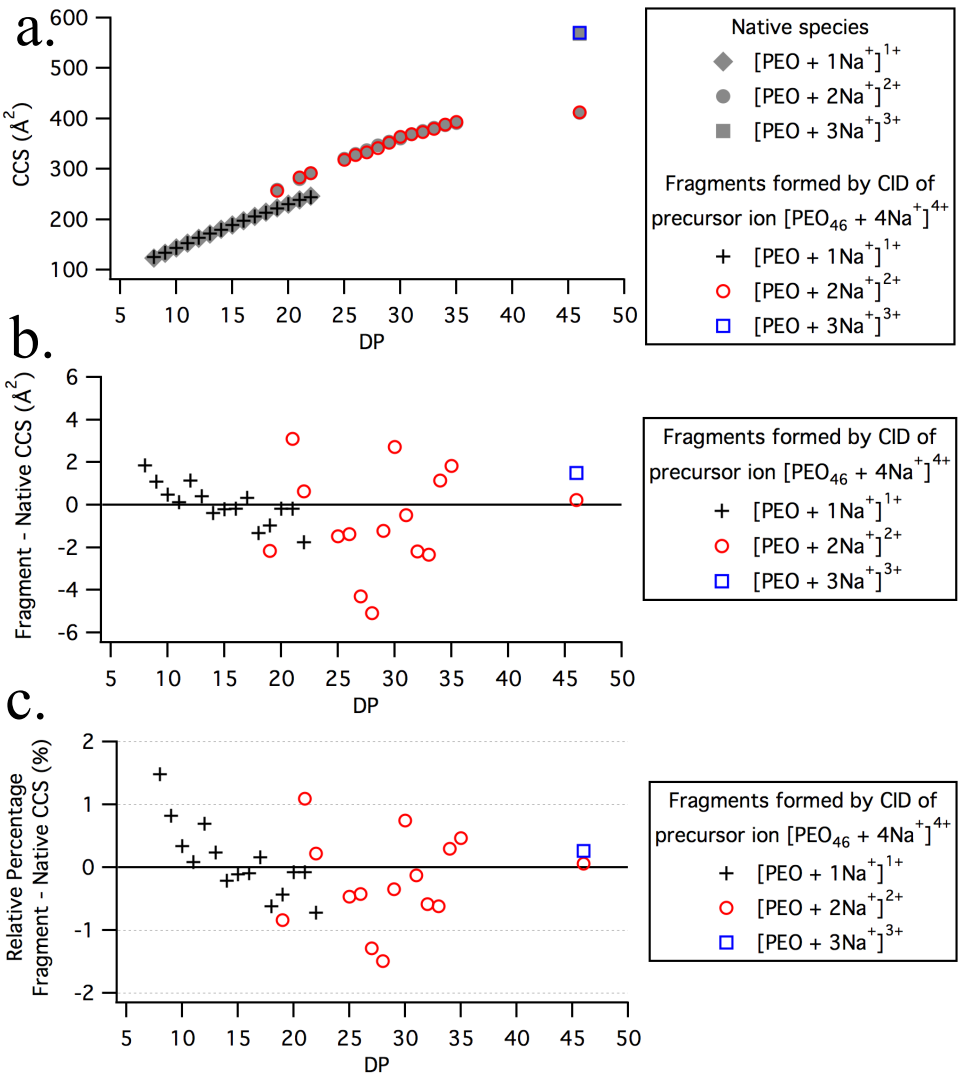

Figure SI11: Comparison of CID-obtained fragment ions from the $[PEO_{46} + 4Na^+]^{4+}$ precursor ion with native intact polymer ions as a function of the DP. The analyzed fragment ions yield *m/z* values identical to smaller intact polymer ions. a. CCS plotted as a function of the DP. Gray markers represent native intact polymer ions and colored markers represent fragment ions. b. CCS difference between fragment ions and native intact polymer ions. c. Percentage CCS deviations of fragment ions and native intact polymer ions (Equation 1 with CCS instead of t_d).

Table SI3: t_d and CCS percentage deviations of fragment ions from $[PEO_{46} + 4Na^+]^{4+}$ compared to their native (intact) counterparts (Equation 1 for either t_d or CCS). The analyzed species correspond to ions having *m/z* values of depolymerized polymer ions, without assuming that the fragment ions are solely formed by depolymerized ions. Figures SI10 and SI11 represent the plots of the t_d and CCS evolutions, their differences and their percentage deviations. The t_d of most fragment ions is beyond the limiting acquisition bin width (Figure SI10.b.).

Fragments from precursor ion $[PEO_{46}+4Na^+]^{4+}$						
DP	$[M+1Na^+]^{1+}$		$[M+2Na^+]^{2+}$		$[M+3Na^+]^{3+}$	
	% dt	% CCS	% dt	% CCS	% dt	% CCS
8	2.27	1.48				
9	1.27	0.82				
10	0.53	0.34				
11	0.14	0.09				
12	1.08	0.69				
13	0.38	0.24				
14	-0.33	-0.21				
15	-0.17	-0.11				
16	-0.15	-0.09				
17	0.25	0.16				
18	-0.98	-0.62				
19	-0.68	-0.43	-1.30	-0.84		
20	-0.12	-0.07				
21	-0.12	-0.08	1.69	1.09		
22	-1.14	-0.72	0.34	0.22		
25			-0.73	-0.47		
26			-0.66	-0.42		
27			-2.02	-1.29		
28			-2.34	-1.49		
29			-0.54	-0.34		
30			1.17	0.75		
31			-0.20	-0.13		
32			-0.92	-0.58		
33			-0.97	-0.61		
34			0.47	0.30		
35			0.73	0.46		
46			0.09	0.06	0.41	0.26

In Figures SI12-SI14, the blue lines correspond to the 95% confidence bands; the red lines correspond to the 95% prediction bands.

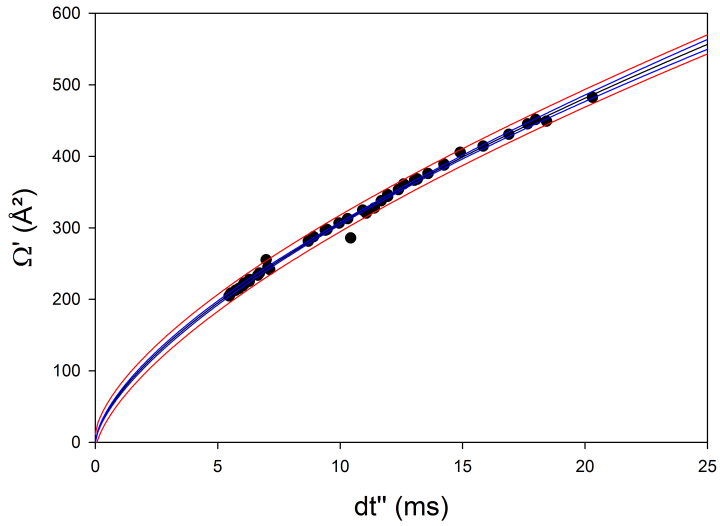

Figure SI12: Traveling wave calibration curve (from drift times to CCS values) for CIU experiments of PEtP. The power fit function is used to establish the calibration curve ($\Omega'=a.dt''^{b}$). The fit parameters of the calibration curve are $a=68.3367$ and $b=0.6516$; the fit parameters of the 95% prediction band are $a=61.6784$ and $b=0.6773$.

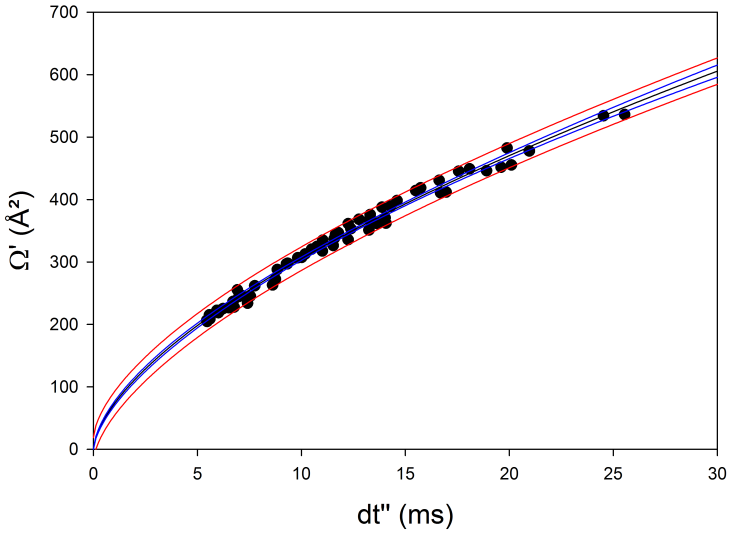

Figure SI13: Traveling wave calibration curve (from drift times to CCS values) for CID experiments of PEtP and PEO. The power fit function is used to establish the calibration curve ($\Omega'=a.dt''^{b}$). The fit parameters of the calibration curve are $a=72.6837$ and $b=0.6234$; the fit parameters of the 95% prediction band are $a=62.1956$ and $b=0.6606$.

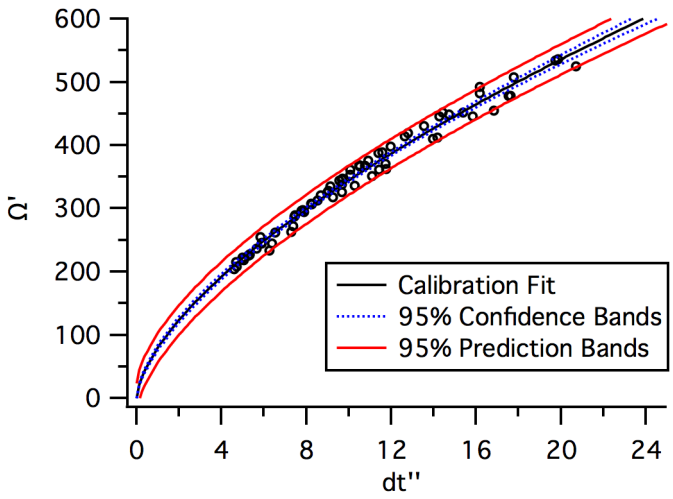

Figure SI14: Traveling wave calibration curve (from drift times to CCS values) for CID experiments of P*n*-PrOx. The power fit function is used to establish the calibration curve ($\Omega'=a.dt''^{b}$). The fit parameters of the calibration curve are $a=79.5086$ and $b=0.6368$; the fit parameters of the 95% prediction band are $a=66.4214$ and $b=0.6826$.

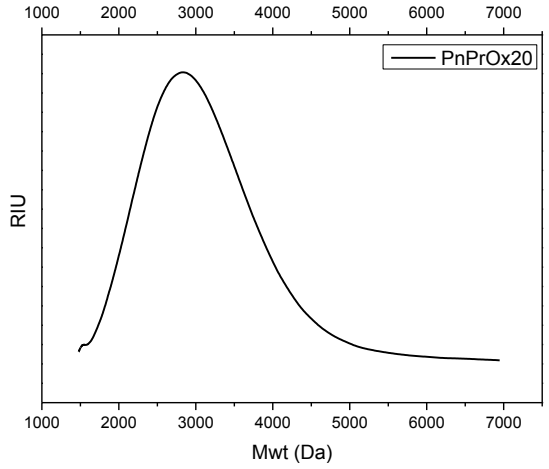

Figure SI15: Molar mass distribution calculated for the P*n*-PrOx polymer as determined by Size Exclusion Chromatography (SEC). Number average molar mass (Mn) = 2600 Da. Dispersity (Đ) = 1.08. Eluent: *N, N*-dimethylacetamide. Molar mass and dispersity values calculated against PMMA standards.